

## Second-Class Currents in $0^- \rightarrow 0^+$ and Unique Nuclear $\beta$ Transitions

B. Eman and D. Tadić

Institute “Rudjer Bošković”, and University of Zagreb, Zagreb, Yugoslavia

F. Krmpotić\*

Departamento de Física, Facultad de Ciencias Exactas, Universidad de La Plata,  
 La Plata, Argentina

L. Szybisz\*\*

Institut für Experimentelle Kernphysik der Universität  
 und des Kernforschungszentrums Karlsruhe, Karlsruhe, Fed. Republic of Germany

Received February 27, accepted February 28, 1975

*Abstract.* The induced pseudotensor contribution to  $0^- \rightarrow 0^+$  and unique  $\beta$  transitions has been analyzed starting from two possible forms of the nonrelativistic Hamiltonian. The role of mesonic corrections and mesonic second-class currents has been discussed.

### I. Introduction

Renewal of the search for second-class currents (SCC) in weak interactions [1] has prompted reinvestigations of the non-relativistic approximation (NRA) for the nuclear  $\beta$ -decay Hamiltonian [2].

The non-relativistic weak Hamiltonian may be written as follows

$$\begin{aligned}
 H_\beta = & g_A \boldsymbol{\sigma} \cdot \mathbf{L}_4 - \frac{g_A}{2M} i\mathbf{V} \cdot \boldsymbol{\sigma} L_4 + \frac{g_A}{M} L_4 \boldsymbol{\sigma} \cdot \mathbf{p} \\
 & + g_V L_2 + \frac{g_V}{2M} (-i\mathbf{V}) \cdot \mathbf{L}_2 + \frac{g_V}{M} \mathbf{L}_2 \cdot \mathbf{p} \\
 & - \frac{g_V}{2M} (\mu_p - \mu_n) (i\boldsymbol{\sigma}) \cdot (\mathbf{V} \times \mathbf{L}_2) + H(IP) + H(IT) \quad (1)
 \end{aligned}$$

\* Member of the Scientific Research Career of the Consejo Nacional de Investigaciones Científicas y Técnicas, Argentina.

\*\* On leave from the Departamento de Física, Facultad de Ciencias Exactas y Naturales, Universidad de Buenos Aires, as Fellow of the Consejo Nacional de Investigaciones Científicas y Técnicas, Argentina.

where  $\mathbf{L}_i$  and  $L_i$  are appropriate combinations of the lepton wave functions as mentioned in Refs. 3, 4;  $g_A$  and  $g_V$  are, respectively, the effective axial vector and vector coupling constants;  $M$  is the nucleon mass and  $\mu_p$  and  $\mu_n$  are the anomalous magnetic moments of proton and neutron, respectively.

The NRA of the induced pseudoscalar interaction  $H(IP)$  has been treated in our earlier papers [3, 4], so we will restrict here our attention to the induced pseudotensor interaction  $H(IT)$ .

There are two possible NRA for the induced pseudotensor interaction [5], namely

$$\begin{aligned}
 H(IT) = & -\frac{Y}{2M} [\rho \boldsymbol{\Omega} \boldsymbol{\sigma} \cdot \mathbf{L}_4 + i\mathbf{V} \cdot \boldsymbol{\sigma} L_4] \\
 & + \frac{Y}{(2M)^2} [\boldsymbol{\Omega} L_4 \boldsymbol{\sigma} \cdot \mathbf{p} - 2i\boldsymbol{\sigma} \cdot \mathbf{V} L_4 \cdot \mathbf{p}] \quad (2)
 \end{aligned}$$

with

$$\rho = 0 \quad (\text{case A})$$

and

$$\rho = 1 \quad (\text{case B}).$$

The symbol  $Y$  stands for the induced pseudotensor coupling constant defined in Ref. 4, while

$$\Omega = W_0 + 2\xi, \quad \xi = \alpha Z/2r_0;$$

$W_0$  is the energy release of the  $\beta$ -decay in units of  $mc^2$ ,  $\alpha$  is the fine structure constant and  $Z$  and  $r_0$  are the charge and nuclear radius of the daughter nuclei.

The physical meaning of the approximations A and B has been discussed in detail in a recent paper [5]. However, it is worthwhile to mention here that the non-relativistic Hamiltonian (2) depends on the assumptions concerning the form of the phenomenological induced pseudotensor Hamiltonian, mesonic effects and nuclear models.

The case B is mainly the approximation used in our previous analysis [3, 4]. However, the terms proportional to  $1/M^2$  in Eq. (2) have been overlooked there. The modifications due to these new terms are indicated in Section II.

As shown in Ref. 6, mesonic SCC can produce an effective single-particle induced pseudotensor as the one appearing in Eq. (2) and, in addition, some two-body transition operators. In the present work these two-body operators are discussed only in the role of effective parameters. We comment mesonic SCC in Section III.

It is demonstrated in Section IV, that the hypothesis of conserved induced pseudotensor current [2], conduces to an interesting relationship between the n.m.e.  $\langle i\boldsymbol{\sigma} \cdot \mathbf{p}/M \rangle$  and  $\langle \boldsymbol{\sigma} \cdot \mathbf{r} \rangle$ .

The search for the induced pseudotensor interaction, performed so far, in the  $0^- \rightarrow 0^+$   $\beta$  transitions, was based on the experimental data, reported by Daniel and Kaschl [7], for the spectrum shape factor in  $^{144}\text{Pr}$  and  $^{166}\text{Ho}$  nuclei. The parameter  $b = Y/g_A$  was required to be rather large and negative.

The unique first forbidden  $\beta$  transitions, measured by Daniel *et al.* [8] ( $^{42}\text{K}$ ,  $^{86}\text{Rb}$ ,  $^{90}\text{Sr}$ ,  $^{90}\text{Y}$ ) and by Beekhuis [9] ( $^{142}\text{Pr}$ ,  $^{166}\text{Ho}$ ) were analysed in Ref. 3. The parameters  $h$  and  $g_T$  used there are connected with our parameter  $Y$  through  $h = g_T = Y/2M$ . These studies show that the experimental spectrum-shape factors can be explained either by,

(i) choosing appropriate values for the higher order (third forbidden) nuclear matrix elements (n.m.e.), when  $b = 0$ , or

(ii) by the n.m.e. calculated in the spherical single-particle shell-model, when  $b \geq 0$ .

Meanwhile, new measurements of the spectrum shape factors of the  $0^- \rightarrow 0^+$   $\beta$  transitions have been reported: by Liaud [10] in  $^{166}\text{Ho}$ , by Nagarajan *et al.* [11] in

$^{144}\text{Pr}$  and by Flothmann *et al.* [12] and Persson *et al.* [13] in  $^{206}\text{Tl}$ . Liaud [10] has also measured the spectrum shape factor of the  $0^- \rightarrow 2^+$  transition in  $^{166}\text{Ho}$ . It appears then necessary to bring our previous works [3, 4] up to date, in accordance with the present level of knowledge. This is done in Section V.

We will concentrate our attention on the  $^{166}\text{Ho}$ , as this nucleus present several interesting features, namely

- both  $0^- \rightarrow 0^+$  and  $0^- \rightarrow 2^+$  transitions occur;
- in addition to the experimental information about the spectrum shape-factors, also the data for the  $0^- \rightarrow 2^+ \rightarrow 0^+$   $\beta-\gamma$  angular correlation are available [14];
- the structure of the states involved in the  $\beta$ -decay processes is fairly well known.

Finally, in Section VI the conclusions are presented. The results for forbidden transitions are contrasted with those for allowed transitions to see whether any general pattern emerges. In fact, if the effective induced pseudotensor is present, all deviations from the "normal" spectrum shapes should be explainable in terms of the parameter  $b = Y/g_A$  fixed from allowed  $ft$  values [5].

## II. Spectrum-Shape Factors for $0^- \rightarrow 0^+$ and Unique Nuclear $\beta$ -Transitions

A detailed description of the formalism for different  $\beta$ -decay observables can be found in Refs. 3, 4; here we simply sketch the procedure and give the pertinent definitions for the spectrum shape factors.

From the comparison of the expressions (1) and (2) it can be easily seen that the first three induced pseudotensor terms will contribute to the shape factor in the same way as the corresponding axial vector terms. The contribution coming from the last term in Eq. (2) is worked out in the Appendix.

The spectrum-shape factor for  $0^- \rightarrow 0^+$  transitions is of the form [4]

$$C_\beta^0(W) = \frac{g_A^2 |\langle \boldsymbol{\sigma} \cdot \mathbf{r} \rangle|^2}{2p^2 q^2 F_0(Z, W)} \sum_{\kappa=-1}^1 |C_0(\kappa)|^2 \quad (3)$$

where  $p$  and  $q$  are electron and neutrino momenta, respectively, and  $F_0(Z, W)$  is the Fermi function. The coefficients  $C_0(\kappa)$ , including the induced pseudotensor interaction, are:

$$\begin{aligned} C_0(1) = & \left( 1 - \rho \frac{b\Omega}{2M} \right) (f_1 F_{-1} - g_1 F_1) r_0^{-1} \\ & + \left( 1 + \frac{b\Omega}{4M} \right) f (f_1 F_1 + g_1 F_{-1}) + \frac{(1+b)}{2M} \\ & \cdot \left[ \Omega (f_1 F_{-1} - g_1 F_1) + (g_1 F_1 + f_1 F_{-1}) - \left( \frac{4}{r_0} \right) g_1 F_{-1} \right] r_0^{-1} \end{aligned}$$

$$\begin{aligned}
& + f \frac{b}{6M} [\Omega(f_1 F_1 + g_1 F_{-1}) + (f_1 F_1 - g_1 F_{-1})] \\
C_0(-1) & = \left(1 - \rho \frac{b\Omega}{2M}\right) (g_{-1} F_{-1} + f_{-1} F_1) r_0^{-1} \\
& + \left(1 + \frac{b\Omega}{4M}\right) f(g_{-1} F_1 - f_{-1} F_{-1}) \\
& + \frac{(1+b)}{2M} \left[ \Omega(g_{-1} F_{-1} + f_{-1} F_1) + (f_{-1} F_1 - g_{-1} F_{-1}) \right. \\
& \left. + \left(\frac{4}{r_0}\right) f_{-1} F_{-1} \right] r_0^{-1} \\
& + f \frac{b}{2M} [\Omega(g_{-1} F_1 - f_{-1} F_{-1}) - (g_{-1} F_1 + f_{-1} F_{-1})] \quad (4)
\end{aligned}$$

with

$$f = \frac{\langle i \boldsymbol{\sigma} \cdot \mathbf{p} \rangle}{M \langle \boldsymbol{\sigma} \cdot \mathbf{r} \rangle}. \quad (5)$$

Here  $f_\kappa$  and  $g_\kappa$  are the electron wave functions and the  $F_\kappa$  are the neutrino ones.

From the above expressions we see that in the case B the induced pseudotensor contributions cancel partially out.

In the case of unique transitions, in addition to the induced pseudotensor interaction, also, the induced tensor interaction, as well as the higher order terms in the multipole expansion of the weak Hamiltonian, can contribute. The shape factor is now

$$C_\beta^2(W) = \frac{2}{p^2 q^2 F_0(Z, W)} \frac{g_A^2 |\langle r T_{21} \rangle|^2}{25 r_0^2} \sum_{\kappa=-2}^2 |C_2(\kappa)|^2, \quad (6)$$

where the coefficients  $C_2(\kappa)$  are

$$\begin{aligned}
C_2(\kappa) & = \left(1 - \rho \frac{b\Omega}{2M}\right) A_\kappa + \frac{1}{M} (1+b) B_\kappa \mp \frac{3}{2M} C_\kappa \\
& + \alpha_2 \left[ D_\kappa + \frac{1}{M} (1+b) E_\kappa \pm \frac{c}{M} F_\kappa \right] + \left(1 + \frac{b}{4M}\right) \alpha_3 G_\kappa \\
& + \alpha_4 H_\kappa + \alpha_5 I_\kappa, \quad (7)
\end{aligned}$$

in which the upper and lower signs corresponds to  $\kappa=1, 2$  and  $\kappa=-1, -2$ , respectively. The quantities  $A_\kappa, B_\kappa, C_\kappa, D_\kappa, E_\kappa, F_\kappa, G_\kappa$  and  $H_\kappa$  are defined in Ref. 3 and are functions of the electron and neutrino wave functions. The coefficients  $I_\kappa$  are originated by the last term in Eq. (2) and are related to the coefficients  $A_\kappa$  by the expression

$$I_\kappa = -\frac{b}{6M} \left( \frac{d}{dr} + \frac{2}{r} \right) A_\kappa. \quad (8)$$

The meaning of the other symbols is

$$c = (\mu_p - \mu_n) \frac{g_V}{g_A} = 4.7 \frac{g_V}{g_A}, \quad (9)$$

$$\begin{aligned}
\alpha_2 & = \sqrt{\frac{3}{2}} \frac{\langle r^3 T_{23}(\hat{r}) \rangle}{r_0^2 \langle r T_{21}(\hat{r}) \rangle}, \quad \alpha_3 = \sqrt{10} \frac{\langle i Y_2 r^2 \boldsymbol{\sigma} \cdot \mathbf{p} \rangle}{M r_0 \langle r T_{21}(\hat{r}) \rangle}, \\
\alpha_4 & = \frac{g_V}{g_A} \sqrt{15} \frac{\langle i r^2 p T_{22}(\hat{p}) \rangle}{M r_0 \langle r T_{21}(\hat{r}) \rangle}, \quad \alpha_5 = \frac{r_0 \langle i p T_{21}(\hat{p}) \rangle}{\langle r T_{21}(\hat{r}) \rangle}. \quad (10)
\end{aligned}$$

In the above expressions it has been assumed that  $r$ -dependent lepton wave functions can be taken out of the n.m.e. However, in the region of relatively large  $ft$  values, this approximation might be very bad and it is necessary to consider explicitly the effects of additional n.m.e. which arise from the expansion of the lepton wave-functions in powers of  $r^2$ . Here we will use the formalism presented in Refs. 3, 4, which leaves us with the smallest possible number of additional parameters, namely with the ratios

$$\alpha_1 = \frac{\langle r^3 T_{21}(\hat{r}) \rangle}{r_0^2 \langle r T_{21}(\hat{r}) \rangle} \quad (11)$$

in the case of unique transitions and with

$$\varepsilon_1 = \frac{\langle r^2 \boldsymbol{\sigma} \cdot \mathbf{r} \rangle}{r_0^2 \langle \boldsymbol{\sigma} \cdot \mathbf{r} \rangle} \quad \text{and} \quad \varepsilon_2 = \frac{\langle r^2 \boldsymbol{\sigma} \cdot \mathbf{p} \rangle}{r_0^2 \langle \boldsymbol{\sigma} \cdot \mathbf{p} \rangle} \quad (12)$$

in the case of  $0^- \rightarrow 0^+$  transitions. In the independent-particle shell-model the ratios  $\alpha_i$  and  $\varepsilon_i$  are estimated to be

$$\begin{aligned}
\alpha_1 & = \frac{2}{3}, \quad \alpha_2 = -\frac{1}{6}, \quad \alpha_3 = \frac{3}{2} \xi r_0 A, \\
\alpha_4 & = -\frac{5}{2} \frac{g_V}{g_A} \frac{1}{M r_0}, \quad \alpha_5 = -2 \xi r_0 A, \\
\varepsilon_1 & = \varepsilon_2 = \frac{2}{3}, \quad 1 \leq A \leq 3. \quad (13)
\end{aligned}$$

### III. Mesonic Second-Class Currents

The possibility that SCC may be entirely composed of meson fields was suggested [15] to explain the energy independence of  $ft$  ratios for allowed transitions [16] which was found experimentally. A detailed investigation of single-particle contributions coming from the closed-loop diagram leads to the conclusion [6] that the  $\pi\omega$  loop gives an effective  $H_\beta$  of the form given by Eqs. (1) and (2). Other combinations of mesons, such as  $\rho\omega, K^*K$ , etc., give different closed-loop contributions. However, when the cutoff is introduced and estimated on the basis of  $\Delta S \neq 0$  semileptonic decays [17] the result is comparable with the  $\pi\omega$ -loop contribution. It is obvious that our analysis of forbidden transitions does not yield information about the origin of the parameter  $b$ . The

effect may be entirely due to either mesonic SCC or some other effect, or its origin may be mixed. Mesonic SCC currents can also be exchanged between nucleons, thus leading to two-body transition operators [6, 18]. For  $0^- \rightarrow 0^+$  transitions, the dominant term is [6]

$$D_2 = d_2 L_4 = \frac{\kappa}{2M} [(\boldsymbol{\sigma}_2 \cdot \boldsymbol{V}_2) Q_A \tau_2^\mp + (\boldsymbol{\sigma}_1 \cdot \boldsymbol{V}_1) Q_A \tau_1^\mp] L_4, \quad (14)$$

where

$$Q_A = \frac{1}{(m_\omega^2 - m_\pi^2) 8 \pi^3} \cdot \int d^3 k e^{i\mathbf{k} \cdot (\mathbf{r}_1 - \mathbf{r}_2)} \left[ \ln \left( \frac{k^2 + m_\omega^2}{k^2 + m_\pi^2} \right) - \frac{m_\omega^2 - m_\pi^2}{k^2 + m_\omega^2} \right]. \quad (15)$$

This term can be included in our formalism as a redefinition of the parameter  $f$

$$\hat{f} = \left\langle \frac{i \boldsymbol{\sigma} \cdot \mathbf{p}}{M} + d_2 \right\rangle / \langle \boldsymbol{\sigma} \cdot \mathbf{r} \rangle. \quad (16)$$

The theoretical calculation of the single-particle n.m.e. ratio  $f$  is a rather difficult task [19]. We can even less hope for a reliable estimate of the two-body matrix element  $\langle d_2 \rangle$ . As the mesonic SCC coupling constant has to be small, the modification of  $f$  presented by Eq. (16) is probably not very important. Our analysis does not distinguish  $f$  from  $\hat{f}$ .

Two-body transition operators for unique transitions are by far more complex. Most of the operators appearing in the n.m.e. ratios  $\alpha_i$  receive two-body operators as additions. As we have estimated only single-particle contributions, our analysis would be at best an approximation.

#### IV. Conserved Second-Class Axial-Vector Current

In the next section we present a phenomenological search for SCC effects. However, the physics associated with SCC is not completely contained in the terms multiplied by the constant  $b$ . Let us show how we can find relations among n.m.e. through the concept of conserved second-class axial-vector current (CSAC). This concept was introduced in Ref. 2 when evaluating two-body exchange corrections to the single-particle induced pseudotensor term. Here we want to use this concept in close analogy to the explanation of the problem of conserved vector current (CVC) [20, 21].

Writing the induced pseudotensor interaction as

$$H_{\text{int}}(IT) = (IT)_\mu L_\mu, \quad (17)$$

where

$$L_\mu = (i \mathbf{L}_4, L_4), \quad (18)$$

we find for case A

$$(IT)_\mu = \frac{Y}{2M} \left( -(\boldsymbol{\sigma} \cdot \boldsymbol{V}) \frac{\mathbf{p}}{M}, -i \boldsymbol{\sigma} \cdot \boldsymbol{V} + \frac{\Omega}{2M} \boldsymbol{\sigma} \cdot \mathbf{p} \right). \quad (19)$$

The rest then closely follows the standard Refs. 20, 21 or books [22]. The nuclear wave functions in expression (19) should be understood, and one has to study the nuclear matrix element

$$\int \boldsymbol{V} \cdot (\mathbf{IT}) f_i(r, \theta, \phi) d\tau = - \int (\mathbf{IT}) \cdot \boldsymbol{V} f_i(r, \theta, \phi) d\tau. \quad (20)$$

Here  $f_i(r, \theta, \phi)$  are some suitable coordinate functions, the derivative of which leads to the required  $\beta$ -decay n.m.e. The functions  $f_i$  appear naturally in the expansion of the lepton wave-function bilinears  $\mathbf{L}_4$  and  $L_4$ . The relation

$$\partial_\mu (IT)_\mu = 0 \quad (21)$$

together with the gauge-invariant substitution  $\partial_\mu \rightarrow \partial_\mu - i e A_\mu$  then leads to the n.m.e. relation

$$\begin{aligned} \langle f | (\boldsymbol{\sigma} \cdot \boldsymbol{V}) \frac{\mathbf{p} \cdot \boldsymbol{V}}{M} f_i | i \rangle \\ \cong (W_0 + 2\xi) \langle f | \left[ -i \boldsymbol{\sigma} \cdot \boldsymbol{V} + \frac{\Omega}{2M} \boldsymbol{\sigma} \cdot \mathbf{p} \right] f_i | i \rangle. \end{aligned} \quad (22)$$

When assessing the physical significance of the outlined approach, one should keep in mind that for the single-particle induced pseudotensor of the form

$$H_{\text{int}}(IT) = - \frac{Y}{2M} \frac{1}{2} [\gamma_\mu, \gamma_\nu] - \gamma_5 \partial_\nu L_\mu \quad (23)$$

relation (21) is obviously an identity. However, the two-body exchange contribution can be considered as included in Eqs. (21) and (22).

Choosing

$$f_i = r^2 \quad (24)$$

and neglecting the second term on the r.h.s. of Eq. (22), one obtains for  $0^- \rightarrow 0^+$  transitions

$$\left\langle \frac{i \boldsymbol{\sigma} \cdot \mathbf{p}}{M} \right\rangle \cong (W_0 + 2\xi) \langle \boldsymbol{\sigma} \cdot \mathbf{r} \rangle. \quad (25)$$

It is interesting that the predicted n.m.e. ratio  $f$  is in qualitative agreement with experimental results. Eq. (25) resembles the Ahrens-Feenberg formula [23, 24]\*

\* The analogous formula from  $\langle f | i \mathbf{p} / M | i \rangle = (W_0 + 2\xi) \langle f | \mathbf{r} | i \rangle$  corresponds in the same way to the Ahrens-Feenberg formula

$\langle f | i \mathbf{p} / M | i \rangle \cong (W_0 + \xi) \langle f | \mathbf{r} | i \rangle.$

$$\left\langle \frac{i\boldsymbol{\sigma} \cdot \mathbf{p}}{M} \right\rangle \cong (W_0 + \zeta) \langle \boldsymbol{\sigma} \cdot \mathbf{r} \rangle. \quad (26)$$

It is questionable whether one is allowed to repeat the same trick for case B. For this case the concept of CSAC has already been employed in deriving the effective  $H_{\text{int}}$ . It is not surprising that the condition (21) applied once more should lead to inconsistency. In the case of  $0^- \rightarrow 0^+$  transitions, for example, one deduces

$$\langle f | \frac{\boldsymbol{\sigma} \cdot \mathbf{p}}{M} | i \rangle \cong \frac{\Omega}{4} \langle f | r^2 \frac{\boldsymbol{\sigma} \cdot \mathbf{p}}{M} | i \rangle. \quad (27)$$

As  $\Omega r_0^2/4 \ll 1$ , expression (27) is inconsistent.\* The discussion presented in this section is not applicable to mesonic SCC.

## V. Analysis of the Experimental Data

The method for searching the values of the free parameters was based on the minimization of the reduced chi-square function  $\chi^2$  defined as

$$\chi^2(K) = \frac{1}{N(K)} \sum_{i=1}^{N(K)} \{ [Q_{\text{th}}^K(i) - Q_{\text{exp}}^K(i)] / \Delta Q_{\text{exp}}^K(i) \}^2 \quad (28)$$

where  $N(K)$  is the total number of the experimental values of the observable  $K$ ;  $Q_{\text{exp}}^K(i)$ ,  $\Delta Q_{\text{exp}}^K(i)$  and  $Q_{\text{th}}^K(i)$  are, respectively, the experimental value, the experimental error and the theoretical value of the observable  $K$  at a given energy  $W(i)$ .

The minimization procedure was carried out with the aid of the package of subroutines MINUITs, kindly provided by CERN.

The differences between the nonrelativistic approximations A and B are illustrated in Tables 1 and 2 for  $0^- \rightarrow 0^+$  and unique transitions, respectively. In these calculations Eq. (4) and (7) were considered, while the parameters  $f$  and  $b$  were varied in the region

$$|f| \leq 50, \quad |b| \leq 50. \quad (29)$$

The values of the ratios  $\alpha_2$ ,  $\alpha_3$ ,  $\alpha_4$  and  $\alpha_5$  were those given by Eq. (13).

Table 1. Values of the matrix-element ratio  $f = \left\langle \frac{i\boldsymbol{\sigma} \cdot \mathbf{p}}{M} \right\rangle / \langle \boldsymbol{\sigma} \cdot \mathbf{r} \rangle$  and the coupling constant  $b$  for the spectrum shapes measured by Daniel and Kaschl [7]

	Case A			Case B				
	$f$	$b$	$\chi^2$	$\langle \boldsymbol{\sigma} \cdot \mathbf{r} \rangle$	$f$	$b$	$\chi^2$	$\langle \boldsymbol{\sigma} \cdot \mathbf{r} \rangle$
				$r_0$				$r_0$
$^{144}\text{Pr}$	10.4	-13.0	2.68	1.38	11.6	-13.7	2.68	1.15
$^{166}\text{Ho}$	13.6	-8.7	2.56	0.34	14.6	-8.3	2.56	0.34

\* For  $^{144}\text{Pr}$ ,  $\Omega r_0^2/4 \cong 2.2 \times 10^{-3}$ .

Table 2. Parameter  $b = Y/g_A$  extracted for case A and B from the experimental shapes for unique transitions

	Case A		Case B	
	$b$	$\chi^2$	$b$	$\chi^2$
$^{42}\text{K}^a$	14.9	1.04	17.0	1.02
$^{86}\text{Rb}^a$	2.30	0.22	2.65	0.22
$^{90}\text{Sr}^a$	1.25	3.20	1.50	3.13
$^{90}\text{Y}^a$	-4.42	2.45	-4.72	2.47
$^{142}\text{Pr}^b$	0.55	1.28	0.73	1.27
$^{166}\text{Ho}^b$	18.5	1.26	34.0	1.26

<sup>a</sup> Measurements by Daniel *et al.* [8].

<sup>b</sup> Measurements by Beekhuis [9].

Table 3. Parameters and the coupling constant for the spectrum shapes for  $0^- \rightarrow 0^+$  transitions for case B analyzed in approximation E from Ref. 4. A fourparameter variation has been performed

	$f$	$b$	$\varepsilon_1$	$\varepsilon_2$	$\chi^2$
$^{144}\text{Pr}$	20.9	1.87	2.0	$1.1 \times 10^{-3}$	28.2
$^{166}\text{Ho}$	20.0	1.63	$3 \times 10^{-5}$	1.36	2.55

From the Tables 1 and 2 it can be seen that, while for the  $0^- \rightarrow 0^+$  transitions the approximations A and B give almost identical results for the coupling constant  $b$ , in the case of unique transitions a larger value of  $b$  is needed for the approximation B than for the approximation A.

A second step was taken in order to ascertain whether the results of Daniel and Kaschl are explainable with a positive value of the coupling constant  $b$ , by varying, in addition to  $f$  and  $b$ , also the ratios  $\varepsilon_1$  and  $\varepsilon_2$  with the condition

$$|f| \leq 50, \quad 0 \leq b \leq 50, \quad |\varepsilon_1| \leq 2 \quad \text{and} \quad |\varepsilon_2| \leq 2. \quad (30)$$

The results presented in Table 3 show that, if only  $b > 0$  is allowed, it is not possible to reproduce satisfactorily the experimental data for  $^{144}\text{Pr}$  nucleons, while the ratio  $\varepsilon_1$  needs to be extremely small for  $^{166}\text{Ho}$  isotope.

The analysis of the recent measurements of the  $0^- \rightarrow 0^+$   $\beta$ -transitions has been done in the case A and with  $\varepsilon_1 = \varepsilon_2 = 1$ . The results are shown in Figs. 1, 2a and 2b. The spectrum shape of the  $^{144}\text{Pr}$  nucleons seems to allow both  $b > 0$  and  $b < 0$  including  $b = 0$ , while  $|f| < 40$ . Similar conclusions may be drawn from the two measurements [12, 13] of  $0^- \rightarrow 0^+$  transition in  $^{206}\text{Tl}$ . However, these data seem to be in rather poor mutual agreement.

An extensive analysis was performed on the shape factor measurements, reported by Liaud [10], for both  $0^- \rightarrow 0^+$  and  $0^- \rightarrow 2^+$   $\beta$ -transitions in the  $^{166}\text{Ho}$  nucleons. In addition the  $\beta$ - $\gamma$  angular correlation experiment [14] was also considered.

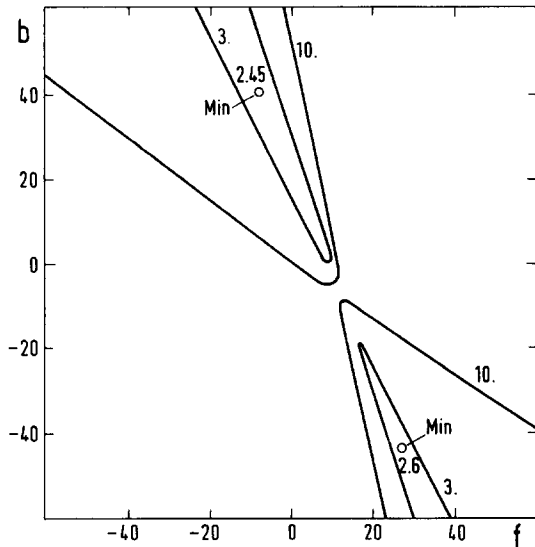


Fig. 1. The  $\chi^2(C_\beta^0)$  plot for the  $0^- \rightarrow 0^+$  transition in  $^{144}\text{Pr}$  (case A). The measurement performed by Nagarajan *et al.* [11] was analyzed

The above mentioned data were fitted simultaneously [25] by minimizing the total  $\chi^2$ -function

$$\chi_T^2 = \chi^2(C_\beta^0) + \chi^2(C_\beta^2) + \chi^2(\varepsilon_{\beta\gamma}). \quad (31)$$

The results, summarized in Table 4, were obtained by varying the parameters  $f$  and  $b$  (in runs Nos. 1, 2, 3, 4, 7 and 8) or  $\alpha_1$  (run No. 6) between the limits

$$|f| \leq 50 \quad \text{and} \quad |b| \leq 50 \quad (\text{or} \quad |\alpha_1| \leq 2). \quad (32)$$

In the run No. 5, only the ratio  $f$  was considered as a free parameters. The ratios  $\varepsilon_i$  and  $\alpha_i$  were fixed on the basis of the single-particle spherical shell model estimates (see Eq. (13)) and from the Nilsson model. In the second case, the initial intrinsic states are taken to be  $7/2^- [523 \uparrow]$  and  $7/2^+ [633 \uparrow]$  for the odd proton and odd neutron, respectively, while in the final state both protons are in the  $7/2^- [523 \uparrow]$  state. The formulas quoted in Refs. 26–28 were used with the deformation parameter  $\delta = 0.3$ .

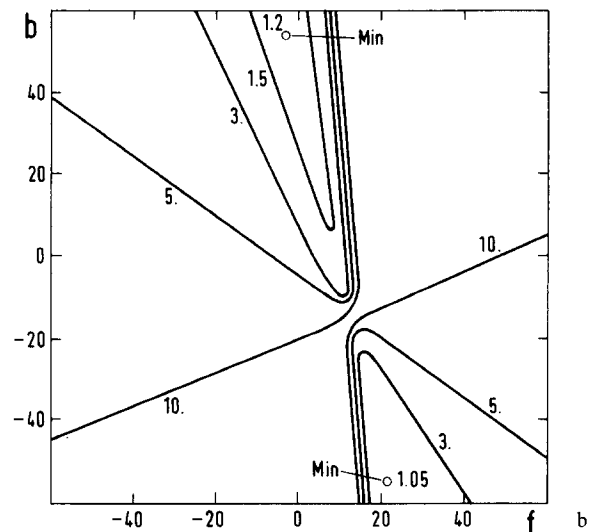
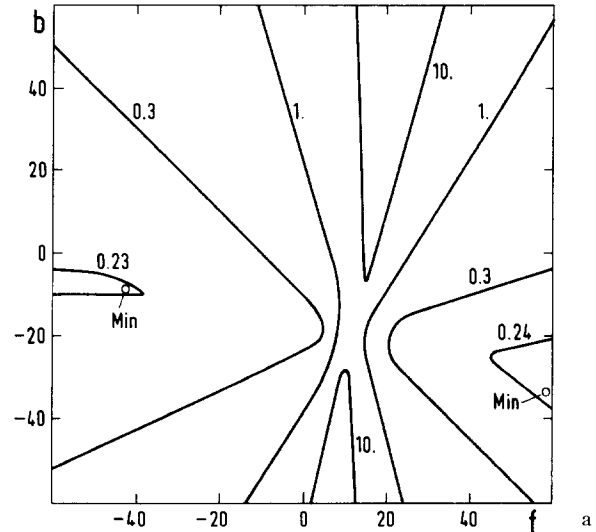


Fig. 2a and b. The  $\chi^2(C_\beta^0)$  plot for the  $0^- \rightarrow 0^+$  transition in  $^{206}\text{Tl}$  (case A). The results of the analysis of the measurements performed by Flothmann *et al.* [12] and Persson *et al.* [13] are displayed in (2a) and (2b), respectively

Table 4. Analysis of  $^{166}\text{Ho}$ . The ratios of n.m.e. are estimated from the single-particle spherical (see Eq. (13)) and deformed (Nilsson) shell models. The ratio  $\alpha_5$  is taken always to be  $\alpha_5 = -4/3\alpha_3$

No.	Case	$f$	$b$	$\chi^2(C_\beta^0)$	$\chi^2(C_\beta^2)$	$\chi^2(\varepsilon_{\beta\gamma})$	$\langle \sigma \cdot r \rangle$	$\langle r T_{21} \rangle$	$\varepsilon_1$	$\varepsilon_2$	$\alpha_1$	$\alpha_2$	$\alpha_3$	$\alpha_4$
							$r_0$	$r_0$						
1	A	23.53	28.32	0.35	1.01	0.28	0.055	0.275	1	1	1	-0.166	0.7	0.095
2	B	18.56	21.03	0.35	1.01	0.28	0.071	0.337	1	1	1	-0.166	0.7	0.095
3	A	22.54	25.18	0.39	1.01	0.27	0.056	0.300	0.748	0.452	0.744	0.390	0.193	0.475
4	B	18.26	18.50	0.39	1.01	0.27	0.074	0.381	0.748	0.452	0.744	0.390	0.193	0.475
5	B	15.6	0	0.52	3.55	0.16	0.177	0.412	1	1	1	-0.166	0.7	0.097
6	B	15.6	0	0.54	0.90	0.41	0.175	0.771	1	1	0.191	-0.166	0.7	0.097
7	A	20.2	16.53	0.37	0.99	0.28	0.077	0.374	1	1	0.666	-0.166	0.7	0.097
8	B	18.7	24.14	0.35	1.01	0.28	0.067	0.376	1	1	1	0	0	0

It is interesting to note that the Nilsson model predicts the following general expression for the ratio  $f$ ,

$$f = \omega_0 \simeq 80 A^{-1/3} \quad (33)$$

being  $\omega_0$  the frequency of the nuclear harmonic oscillator potential.

There are some particular note worthy features in the results presented in Table 4. Firstly, the spectrum shape factor of the  $0^- \rightarrow 0^+$  transition is satisfactory explained without any induced pseudotensor interaction. Secondly, the shape factor of the  $0^- \rightarrow 2^+$  transition is very sensitive to the ratio  $\alpha_1$ , as it is illustrated by runs Nos. 1, 6 and 7. Thirdly, the measurements of the  $\beta$ - $\gamma$  directional correlation and of the spectrum shape factor for the  $0^- \rightarrow 2^+$  transition seem to be inconsistent with each other.

## VI. Final Remarks

Since for the two groups of forbidden transitions under consideration, nuclear physics theories are not yet sufficiently advanced to determine n.m.e. accurately, the analysis of the first forbidden  $\beta$ -decay transitions was performed on a tentative basis. It should be remembered that even in those cases in which the structure of the nuclear states involved in the process is rather well interpreted, within the framework of conventional models, the calculated n.m.e. represent only a rough estimate of their real values [29]. This is due to the fact that the  $\beta$ -decay n.m.e. depend in a sensitive way of the particle-hole correlations induced by the isospin-dependent residual interactions, which are not well known at all.

Although the present analysis includes much more experimental data than our previous studies [3, 4], the final conclusions are essentially the same, namely that the  $0^- \rightarrow 0^+$  transitions favour  $b < 0$  while most of the unique transitions require  $b > 0$ . This result is valid for both NRA of the induced pseudotensor interaction.

One should keep in mind that i) the experimental data for the  $ft$  values in allowed transitions can be explained with both  $b < 0$  and  $b > 0$ , depending on the NRA, namely  $b > 0$  for case A and  $b < 0$  for case B and ii) the  $\beta$ - $\gamma$  directional correlations in allowed processes do not depend on the NRA and the corresponding measurements are only consistent with  $b \geq 0$  [5].

We can construct mixed second-class interaction models, containing both mesonic SCC and the phenomenological induced pseudotensor [6, 18]. However, the inconsistency of the sign of  $b$  as found for  $0^- \rightarrow 0^+$  transitions with the one required by allowed and unique transitions, can only with difficulty be reconciled with the existence of mesonic SCC.

It should be stressed that our conclusion for the  $0^- \rightarrow 0^+$  transitions ( $b < 0$ ) is mainly based in the measurements of Daniel and Kaschl [7] for  $^{144}\text{Pr}$  and  $^{166}\text{Ho}$ , which can not be satisfactorily explained ( $\chi^2 \leq 1$ ) with any value of  $b$ . On the other hand, Liaud's results [10] for  $^{166}\text{Ho}$  and those of Flothmann *et al.* [12] for  $^{206}\text{Tl}$  are compatible with  $b \geq 0$ . Thus it could be that the experiments reported in Ref. 7 are wrong to such an extent that there is no need at all for a negative value of  $b$ .

The possibility that no  $b$  is required, i.e.,  $b=0$ , if definitely confirmed, most likely precludes the existence of mesonic SCC. It is possible to build up mixed theories in which there is no single-particle induced pseudotensor contributing to (1), but  $d_2$  does exist in Eq. (16). Such conjectures are very inattractive. As their consequences are experimentally almost unobservables, they might be superfluous.

Clearly, it is extremely important that the shape factors of the  $0^- \rightarrow 0^+$  transitions should be carefully remeasured. In addition, more detailed measurements and analysis of the spectrum shape factors in unique transitions and of the  $\beta$ - $\gamma$  directional correlations in allowed transitions would also help to clarify things.

The overall situation must be regarded as considerably uncertain. However, we do feel that more accurate experimental results on the nuclear  $\beta$ -decay processes, completed with a better knowledge of nuclear structure problems, could lead to further information on the presence of SCC in the weak Hamiltonian.

## Appendix

In both cases A and B a new type of the term appeared

$$T_x = (\boldsymbol{\sigma} \cdot \mathbf{V})(\mathbf{L}_4 \cdot \mathbf{p}). \quad (\text{A.1})$$

It can be calculated by applying the standard techniques, starting from the form

$$T_x = (\boldsymbol{\sigma} \cdot \mathbf{V}) \sum_{JM} (1 \nu \lambda m | 1 \lambda JM) p_1^y Y_\lambda^m \Phi_{\lambda J}(r). \quad (\text{A.2})$$

Here,  $\Phi_{\lambda J}(r)$  and  $Y_\lambda^m$  are the radial and angular part of the lepton covariant  $L_4$ , which can be found, for example, in Ref. 30. The momentum operator  $p_1$  acts only on the nuclear wave functions. The notation for the vector coupling coefficient has the usual meaning. After performing the derivation, one obtains

$$T_x = \sum (-)^e \sigma_1^{-e} (1 \nu \lambda m | 1 \lambda JM) p_1^y \cdot \left[ \left( \frac{\lambda+1}{2\lambda+3} \right)^{1/2} (1 \varepsilon \lambda m | 1 \lambda \lambda+1 m+\varepsilon) Y_{\lambda+1}^{m+\varepsilon} D_-(\lambda) \Phi_{\lambda J}(r) - \left( \frac{\lambda}{2\lambda+1} \right)^{1/2} (1 \varepsilon \lambda m | 1 \lambda \lambda-1 m+\varepsilon) Y_{\lambda-1}^{m+\varepsilon} D_+(\lambda) \Phi_{\lambda J}(r) \right]. \quad (\text{A.3})$$

Here

$$D_-(\lambda) = \frac{d}{dr} - \frac{\lambda}{r},$$

$$D_+(\lambda) = \frac{d}{dr} + \frac{\lambda+1}{r}, \quad (\text{A.4})$$

and the summation goes over  $J$  and over the magnetic quantum numbers.

The main contribution to  $0^- \rightarrow 0^+$  transitions comes from the second term in (A.3) when  $J=0$  and  $\lambda=1$  are selected, leading to

$$T_x(0^- \rightarrow 0^+) = -\frac{\sigma \cdot \mathbf{p}}{3} D_+(\lambda=1) \Phi_{10}(r). \quad (\text{A.5})$$

Further computation is then a matter of routine.

The main contribution to unique transitions comes when  $J=2$  and  $\lambda=1$  are selected, leading to

$$T_x(2^- \rightarrow 0^+) = \frac{1}{3} p T_{21}^{-M}(\hat{p}) D_+(\lambda=1) \Phi_{12}(r). \quad (\text{A.6})$$

The new derivative operator appearing in this formula is of the form

$$i \frac{p}{M} T_{21}^M(\hat{p}) = \frac{1}{M} \left( \frac{3}{4\pi} \right)^{1/2} \sum C_{1\ 1\ m}^{2\ M} \sigma_1^y V_1^m. \quad (\text{A.7})$$

This operator acts on nucleon wave functions.

## References

1. Wilkinson, D.H.: Phys. Letters **31 B**, 447 (1970)  
Wilkinson, D.H., Alburger, D.E.: Phys. Rev. Letters **24**, 1134 (1970)  
Wilkinson, D.H.: Phys. Rev. Letters **27**, 1018 (1971)
2. Delorme, J., Rho, M.: Phys. Letters **34 B**, 238 (1971); Nucl. Phys. B **34**, 317 (1971)
3. Eman, B., Krmpotić, F., Tadić, D., Nielsen, A.: Nucl. Phys. A **104**, 386 (1967)  
Abecasis, S.M., Krmpotić, F.: Nucl. Phys. A **151**, 641 (1970)
4. Krmpotić, F., Tadić, D.: Phys. Rev. **178**, 1804 (1969)
5. Eman, B., Tadić, D., Krmpotić, F., Szybisz, L.: Phys. Rev. C **6**, 1 (1972)
6. Eman, B., Guberina, B., Tadić, D.: Phys. Rev. C **8**, 1301 (1973)
7. Daniel, H., Kaschl, G.Th.: Nucl. Phys. **76**, 97 (1966)
8. Daniel, H., Kaschl, G.Th., Schmitt, H., Springer, K.: Phys. Rev. **136 B**, 1240 (1964)
9. Beekhuis, H.: Phys. Letters **21**, 205 (1966); Thesis, University of Groningen (1967)
10. Liaud, P.: Thesis, University of Grenoble (1969)
11. Nagarajan, T., Ravindranath, M., Venkata Reddy, K.: Nuovo Cim. **3 A**, 699 (1971)
12. Flothmann, D., Löhken, R., Wiesner, W., Rebel, H.: Phys. Rev. Letters **25**, 1719 (1970)
13. Persson, B.I., Plesser, I., Sunier, J.W.: Nucl. Phys. A **167**, 470 (1971)
14. Grenacs, L., Hess, R.: Helv. Phys. Acta **38**, 372 (1965)  
Martin, B., Schmidlin, P., Daniel, H.: Nucl. Phys. **71**, 523 (1965)
15. Lipkin, H.J.: Phys. Letters **34 B**, 202 (1971); Phys. Rev. Letters **27**, 432 (1971)
16. Wilkinson, D.H., Alburger, D.E.: Phys. Rev. Letters **26**, 1127 (1971)
17. Pietschmann, H., Rupertsberger, H.: Phys. Letters **40 B**, 662 (1972)
18. Kubodera, K., Delorme, J., Rho, M.: Nucl. Phys. B **66**, 253 (1973)
19. Spector, R.M., Blin-Stoyle, R.J.: Phys. Letters **1**, 118 (1962)
20. Fujita, J.I.: Phys. Rev. **126**, 202 (1962)
21. Eichler, J.: Z. Physik **171**, 463 (1963)
22. Bohr, A., Mottelson, B.R.: Nuclear Structure, vol. 1, Appendix 3 D, New York: Benjamin 1969
23. Ahrens, T., Feenberg, E.: Phys. Rev. **86**, 64 (1952)
24. Yamada, M.: Prog. Theoret. Phys. **9**, 268 (1953)
25. Szybisz, L.: Thesis, University of Buenos Aires (1972)
26. Alaga, G.: Glasnik Mat.-Fiz i Astr. **12**, 245 (1957)
27. Berthier, J., Lipnik, P.: Nucl. Phys. **78**, 448 (1966)
28. Tuong, N.D., Dulancy, H., Brewer, H.R.: Phys. Rev. **159**, 862 (1967)
29. Szybisz, L., Krmpotić, F., Fariolli, M.A.: Phys. Rev. C **9**, 624 (1974)
30. Alaga, G.: Rendiconti Scuola Inter. Fisica "E. Fermi", XV Corso, p. 100 (1961)

Dr. B. Eman  
Dr. D. Tadić  
Institute "Rudjer Bošković" and University of Zagreb  
P.O.B. 1016  
41001 Zagreb  
Yugoslavia

Dr. F. Krmpotić  
Departamento de Física  
Facultad de Ciencias Exactas  
Universidad de La Plata  
Casilla de Correo No. 67  
La Plata  
Argentina

Dr. L. Szybisz  
Institut für Experimentelle Kernphysik der Universität  
und des Kernforschungszentrums Karlsruhe  
D-7500 Karlsruhe  
Postfach 3640  
Federal Republic of Germany